Cellular Physiology and Biochemistry

Cell Physiol Biochem 2017;43:52-68
DOI: 10.1159/000480317
Published online: August 25, 2017
Accepted: June 15, 2017

Original Paper

Exosomes Derived from Mesenchymal Stem Cells Rescue Myocardial Ischaemia/Reperfusion Injury by Inducing Cardiomyocyte Autophagy Via AMPK and Akt Pathways

Liang Liu[a] Xian Jin[a] Cui-Fen Hu[b] Rong Li[a] Zhong'e Zhou[a] Cheng-Xing Shen[a]

[a]Department of Cardiology, Shanghai Jiao Tong University Affiliated Sixth People's Hospital, Shanghai, [b]Department of Ultrasound, the First Affiliated Hospital of Soochow University, Suzhou, China

Key Words
Mesenchymal stem cell • Exosomes • Autophagy • Cardiomyocytes • Myocardial ischaemia/reperfusion Injury

Abstract:
Background/Aims: Reperfusion after an ischaemic insult might cause infarct extension. Mesenchymal stem cell (MSC)-derived exosomes could attenuate myocardial remodelling in animal models of myocardial ischaemia reperfusion injury (MIRI), and the present study aimed to explore the related mechanisms. ***Methods:*** *In vitro*, rat H9C2 cardiomyocytes (H9C2s) were exposed to H_2O_2. Cell viability was detected by the CCK-8 assay, apoptosis was detected by Annexin V-PE/7-AAD staining, ROS production was detected by fluorescence microscopy and flow cytometry, and apoptosis-related proteins and signalling pathway-related proteins were detected by western blot analysis. Autophagic flux was measured using the tandem fluorescent mRFG-GFP-LC3 assay. MSC-derived exosomes were extracted using the total exosome isolation reagent. Apoptosis, myocardial infarction size, heart function and myocardial LC3B expression were examined in an *in vivo* I/R model by the TUNEL assay, TTC/Evan blue staining, echocardiography and immunohistochemicalstaining, respectively. ***Results:*** *In vitro*, H_2O_2 dose-dependently increased ROS production and cell apoptosis in H9C2s and blocked autophagic flux after 3 h of exposure; autophagy gradually decreased thereafter, and the lowest level was detected at 12 h after exposure. MSC-derived exosomes reduced H_2O_2-induced ROS production and cell apoptosis and enhanced autophagy at 12 h after exposure. In H9C2 cells exposed to H_2O_2 for 12 h, treatment with exosomes enhanced autophagy via the AMPK/mTOR and Akt/mTOR pathways. Likewise, *in vivo* exosome injections in rats that underwent I/R injury significantly reduced apoptosis and the myocardial infarct size and upregulated myocardial LC3B expression as well as improved heart function. ***Conclusions:*** Our results indicate that

L. Liu and X. Jin contributed equally to this work.

Cheng-Xing Shen

Department of Cardiology, Shanghai Jiao Tong University Affiliated Sixth People's Hospital, 600 Yishan Road, Shanghai, 200233 (China)
Tel. +86 18501664545, Fax 021-64701361, E-Mail shenchienx2@hotmail.com

MSC-derived exosomes could reduce MIRI by inducing cardiomyocyte autophagy via AMPK/mTOR and Akt/mTOR pathways.

Introduction

Ischaemic heart disease (IHD) is currently one of the leading causes of death worldwide [1]. Timely reperfusion, the mainstay treatment for IHD, cannot only reduce infarct size but also improve survival for patients with IHD [2]. However, as documented in many clinical and basic studies, reperfusion might also lead to infarct extension [3, 4], which is one of the major components of myocardial ischaemia reperfusion injury (MIRI).

Previous studies have shown that mesenchymal stem cells (MSCs), a type of multipotent progenitor cell, could improve cardiac function in animal IHD models and in IHD patients via multiple mechanisms, including cardiomyocyte differentiation, tissue repair, anti-inflammation and immunosuppression [5]. However, transplanted MSCs have a low survival rate in the host, and only a small proportion of transplanted MSCs could be evidenced in target tissue [6, 7]. Despite these limitations, MSC transplantation still works well in certain circumstances, mainly due to their paracrine effects; it is known that MSCs could secrete a large number of growth factors, cytokines, and chemokines that promote myocardial cell proliferation, reduce apoptosis, improve the ischaemic microenvironment and mobilize endogenous cardiac stem cells [8]. In addition, as with many other cell types, MSCs also secrete exosomes [9], which can fuse with cellular plasma membranes of recipient cells and transport proteins and RNA into these cells, thereby altering their fate via various cellular processes and pathways [9]. Several studies have demonstrated that MSC-secreted exosomes have a myocardial protective effect post myocardial infarction and MIRI [10-12]. Furthermore, exosome therapy has several advantages, including no risk of aneuploidy, a lower rate of immune rejection and being an 'off-the-shelf' therapeutic strategy [11, 13].

Autophagy is an intracellular metabolic self-degradative process in which cytoplasmic proteins and damaged organelles are degraded by lysosomes; the degraded products, such as membrane lipids, proteins, free fatty acids and amino acids further play important roles in normal cell metabolism, energy generation, and cellular survival [14, 15]. Autophagy is also closely involved in the pathogenesis of various heart diseases [16]. A previous study demonstrated that MSC-secreted exosomes improved myocardial viability and attenuated myocardial remodelling after MIRI *in vivo* [11]. However, it remains unknown if MSC-secreted exosomes could also regulate autophagy in a MIRI model. Therefore, the present study investigated whether and how MSC-secreted exosomes regulate cardiomyocyte autophagy *in vitro* in H_2O_2-induced hypoxic H9C2 cells (H9C2s) and *in vivo* in a rat I/R model.

Materials and Methods

Animals

Male SD (4 to 10 weeks old) rats were purchased from Slac Laboratory Animal Co., Ltd. (Shanghai, China) and kept under specific pathogen-free conditions. All animal experiments were approved by the Ethics Committee of Xinhua Hospital, which is affiliated with the Shanghai Jiao tong University School of Medicine in Shanghai, China. The approval number was XHEC-D-2016-019. Guidelines of the Institutional Animal Ethics Committee were followed when carrying out *in vivo* experiments.

Cell isolation and culture

Four-to-six-week-old SD rats were used to isolate bone marrow-derived MSCs. The rats were anaesthetized using pentobarbital (50 mg/kg, intraperitoneal injection) to minimize suffering and sacrificed by cervical dislocation without recovery from anaesthesia. Tibias and femurs then were removed under sterile conditions. The bone ends were cut, and the bone marrow was flushed with PBS (Gibco, Carlsbad, CA,

USA, Cat#8115178) supplemented with 1%–2% foetal bovine serum (FBS, Gibco, Cat#10099-141). The cell suspension was then filtered through a 40-μm strainer (BD Falcon, Franklin Lakes, NJ, USA, Cat#352340). After centrifugation of the filtered suspension at 1, 000 rpm/min for 5 min, the bone marrow cells were cultured in DMEM/F12, (HyClone, Beijing, China, Cat#SH30023.FS) supplemented with 10% FBS and 1% penicillin–streptomycin (Gibco, Cat#C0222). The culture medium was changed on the fifth day to remove non-adherent cells, and the cells were passaged two days later. MSCs were passaged using Trypsin-EDTA (0.25%) (Gibco, Cat#25200-056) and identified by flow cytometry (FCM, BD Biosciences, San Jose, CA, USA). Subsequent experiments used third passage cells.

H9C2 cell lines of rat cardiac origin were purchased from the Shanghai Institute for Biological Science. Cells were cultured in DMEM/Hi (HyClone, Beijing, China, Cat# SH30243.01B) with 10% FBS and 1% penicillin–streptomycin at 37°C in a humid environment containing5% CO_2 and passaged using Trypsin-EDTA.

Cell viability assay

The CCK-8 assay was used to measure H9C2 cell viability. H9C2s (1, 000/well) were seeded in 96-well plates overnight. To detect the negative effects of H_2O_2 (Sigma, St. Louis, MO, USA, Ca#216763) on H9C2 cell viability, cells were incubated with different concentrations (50, 100, 200, and 500 μM) of H_2O_2 for 3 h, 6 h and 12 h; normal culture media were used for the control group.

To detect the beneficial effects of exosomes on H9C2 cell viability, cells were first co-cultured with exosomes (10μg/ml) for 12 h and then exposed to H_2O_2 (500 μM) for 12 h. Another group was only co-cultured with H_2O_2 (500 μM) for 12 h. Normal culture media were used for the control group.

At the prespecified time points, 10μL of CCK-8 solution (DOJINDO, Kumamoto, Japan, Cat#AY-4710P) was added to the cells. After incubation for another 4 h, the optical density (OD) values were determined at 450 nm using a microplate reader (BioTek, Winooski, VT, USA). Each group was tested in triplicate in three replicate wells. Cell viability or the proliferation rate of treated cells was calculated as relative values to the control group.

Reactive oxygen species measurements

CM-H_2DCFDA (Invitrogen, Carlsbad, California, USA, Ca#C6827) was used to measure intracellular ROS production. A total of 5×10^5 H9C2s were seeded in 6-well plates overnight. To measure the ROS production induced by H_2O_2 at different time points, cells were exposed to H_2O_2 (500 μM) for 3 h, 6 h and 12 h. Normal culture media were used for the control group.

To reduce the ROS formation induced by H_2O_2, cells were first co-cultured with NAC (5 mM, Sigma, Ca#1009005) for 1 h and then exposed to H_2O_2 (500 μM) for 12 h. The two groups were analysed as described above.

The exosome-mediated reduction of ROS formation was assessed using similar groups as that in the cell viability experiments.

At the prespecified time points, cells were washed with sterile PBS, and 1 ml of DMEM/Hi culture media containing 5μM CM-H_2DCFDA was added. Cells were incubated at 37°C for an additional 30 min and then washed again; then, 1 ml of PBS was added per well. ROS concentrations were determined by FCM (BD Biosciences, San Jose, CA, USA) and fluorescence microscopy (Leica,Wetzlar, Germany). For FCM detection, each group was tested in triplicate.

Annexin V-PE/7AAD assay

Annexin V-PE/7-ADD (eBioscience, Carlsbad, CA, USA, Cat#559763) was detected by FCM to measure apoptosis in H9C2s. A total of 5×10^5 H9C2s were seeded in 6-well plates overnight.

To show that antioxidants reduce H9C2 cell apoptosis following induction by H_2O_2, similar cell groups as that used in the ROS production reduction by NAC experiments were also used in this experiment. In addition, to assess the exosome-mediated reduction of H9C2 cell apoptosis, similar experimental groups were implemented as described in the experiments evaluating the effects of exosomes on cell viability.

At the prespecified time points, cells were collected, washed twice with ice-cold PBS, and incubated for 15 min in 1X Annexin V Binding Buffer containing 7-AAD-Percp and Annexin V-PE. Finally, apoptosis was detected by FCM and analysed by the FlowJo software (Tree Star Inc., Ashland, OR, USA). Experiments were carried out in triplicate.

Western blot analysis

H9C2s were seeded in 6-cm plates overnight. To detect autophagy marker expression, the following antibodies were used: LC3B (Abcam, Cambridge, England, Ca#ab48394, dilution 1:1, 000), p62 (Abcam, Ca#ab56416, dilution 1:1, 000) and Beclin-1 (Abcam, Ca#ab55878, dilution 1:1, 000); to detect the expression levels of apoptosis-related proteins, the following antibodies were used: Bcl-2 (Abcam, Ca#ab59348, dilution 1:1, 000) and Bax (Abcam, Ca#ab32503, dilution 1:1, 000) following H_2O_2 (500 μM) treatment at different time points (3 h, 6 h and 12 h) and NAC treatment at 12 h. The cell groupings were as described above. To detect changes of autophagic flux in the exosome-treated group, after H9C2s were co-culture with exosomes for 12 h, Baf-A1 (100 nM, Selleck, Houston, Texas, USA, Ca#S1413) was added to the cells an hour before exposure to H_2O_2 (500 μM) for 12 h; the 3 other groups were treated as described. To detect changes in p-AMPK/AMPK (Abcam, Ca#ab3706 and Ca#3759, dilution 1:1, 000), p-Akt/Akt (Abcam, Ca#ab38449 and Ca#8805, dilution 1:1, 000) and p-mTOR/mTOR (Abcam, Ca#ab63552 and Ca#2732, dilution 1:1, 000) expression in the exosome-treated group, after H9C2s were co-cultured with exosomes for 12 h, 3-MA (10μM, Sigma, Ca#M9281) was added to the cells an hour before exposure to H_2O_2 (500 μM) for 12 h; the 3 other groups were treated as described. To assess the two signalling pathways, afterH9C2s were co-cultured with exosomes for 12 h, CC (5μM,Selleck, Ca#S7840) or Akti, (5μM,Selleck,Ca#S7776) was added to the cells an hour before exposure to H_2O_2 (500 μM) for 12 h. The other three groups were treated as described.

At prespecified time points, cells were collected, and cell lysates were prepared. An equal quantity of protein (40-60μg) was resolved by SDS/PAGE and transferred to polyvinylidene difluoride membranes. The blots were blocked with 5% milk in Tris-buffered saline with Tween 20 for 2 h at room temperature and then incubated with primary antibodies overnight at 4°C. The blots were subsequently incubated with secondary antibodies conjugated with horseradish peroxidase (dilution 1:1000) for 1 h at room temperature and detected using a chemiluminescence system (Chemi-DocXRS+; Bio-Rad Laboratories, Hercules, CA, USA). Grey scale values of each blot were measured by ImageJ software, and the intensity of each band was normalized to the loading control GAPDH (Beyotime, Shanghai, China, Cat# AG019, dilution 1:1, 000) or the total target protein. Experiments were carried out in triplicate.

Exosome purification and identification

MSC-derived exosomes were extracted from cells using total exosome isolation reagent (Invitrogen, ca#4478359). MSCs were seeded in 10-cm plates overnight, and the cells reached 80% confluence before use. The cells were washed three times with PBS and cultured with serum-free media (Gibco, Cat#12055091) in a hypoxic (1%) environment for 12 h or 24 h. Twelve or 24 h later, the culture media were collected and centrifuged at 2, 000 g for 30 min, and then, the media were filtered through a 0.2-μm filter (Millipore, Billerica, MA, USA, Ca#SLGP033RB). After the removal of cellular debris, approximately 100 ml of culture media from ten plates was concentrated to 500μl or 600μl using a membrane with a 100 kDa MWCO (Millipore, Ca#UFC910096). Then, the concentrate was transferred to a new tube, and 1/2 of the volume of total exosome isolation reagent was added and mixed well by pipetting until a homogenous solution formed. The homogenous solution was incubated at 4°C overnight and then centrifuged at 4°C at 10, 000 g for 1 h. The supernatant fluid was aspirated and discarded, and the exosomes were resuspended in 20μl of PBS. The exosomes were stored at -80°C until use. The concentration of exosomes was approximately 10μg /10^7 cells, as determined using the BCA assay (Sigma, St. Louis, MO, USA, Ca# BCA1-1KT).

The size distribution and concentration of MSC-derived exosomes were detected using tunable resistive pulse sensing analysis by qNano (Izon Science, Christchurch, New Zealand). The exosomes diluted by PBS at a dilution factor of 100 or calibration particles were passed through the Nanopore at a 47.12-mm stretch with a voltage of 0.76 V. The data were measured using the analysis software Izon Control Suite v.3.3.2.2.2000 (Izon Science).

Internalization of MSC-derived exosomes into H9C2 cells

MSC-derived exosomes were labelled with $PKH_2$6 (Sigma, Ca#$PKH_2$6GL) for 15 min at 37°C in the dark and washed three times in PBS with centrifugation at 100, 000×g at 4°C for 2 h. Then, the labelled exosomes (10μg/ml) were added to the prepared H9C2s for 6 h, 12 h and 24 h. After incubation, the cells were washed once with PBS, and the nucleus of the cells was dyed using PBS containing 4, 969-diamidino-2-phenylindole (DAPI, Sigma, Ca# D9542-5 MG) for 5 min. The uptake of MSC-derived exosomes by H9C2 cells was observed using fluorescence microscopy.

TEM

To evaluate the characteristics of the exosomes, the supernatant fluids of MSCs that were previously exposed to a hypoxic environment for 12 h or 24 h were collected, and the exosomes were extracted as described above. Undiluted exosomes were exposed to 3% formaldehyde and 0.1% glutaraldehyde for 10 min at 37°C. Then, exosomes were loaded onto formvar/carbon-coated grids, contrasted with 2% uranyl acetate and examined by TEM (PHILIP, Amsterdam, Netherlands, ca#CM-120).

To measure the autophagosomes caused by exosomes, H9C2s were seeded and grouped as described above.H9C2 cells were harvested by centrifugation (400 g), sectioned and fixed with glutaraldehyde overnight. After dehydration with cold alcohol, the slides were placed in embedding moulds saturated in propylene oxide and incubated in an oven at 60°C for 48 h. The 70-nm-thin sections were prepared and detected by TEM. A total of 3-5 images per section were examined per group in the three independent experiments.

Autophagic flux measurements

To detect autophagic flux, the mRFP-GFP-LC3 reporter plasmid (1 μL/mL) (Addgene, Cambridge, MA, USA, 21074) was transfected into H9C2s using lipofectamine 2000 (Invitrogen, 11668-019) according to the manufacturer's instructions. Then, the transfected cells were processed and grouped as described above. The cell Images were obtained using Olympus FV1000 laser scanning confocal microscopy (Olympus, Tokyo, Japan), and autophagosome and autolysosome dots were quantified manually in at least 4 different H9C2s per group.

Animal grouping and theI/R injury model

SD rats (n=18) weighing 250–300 g were randomly assigned in equal numbers to three groups (n=6 per group).The three groups were as follows: (1) the sham group, in which a suture was applied to the LAD (left anterior descending coronary artery) of rats without ligation; (2) the I/R group, in which the LAD was ligated for 30 min followed by reperfusion for 2 h; and (3) the I/R with exosome injection group, in which exosomes (5μg) dissolved in 10μl PBS were injected into the anterior and lateral part of the visibly injured region using a Hamilton syringe with a 30-gauge needle5 min prior to reperfusion.

Myocardial I/R injury in SD rats was established as described previously [17]. In brief, rats were anaesthetized by intraperitoneal injection of sodium pentobarbital (30 mg/kg) and ventilated with oxygen using a small animal ventilator. After an incision in the left thorax at the level between the fourth and fifth ribs, the heart was exposed, and a 6–0 silk suture slipknot was placed around the proximal LAD. Successful myocardial infarction injury was confirmed by the blanched appearance of the ligation region and marked arrhythmia. Thirty minutes later, the slipknot was removed. Successful reperfusion was confirmed by epicardial hyperaemia. After 2 h of reperfusion, the rats were sacrificed, and the heart was rinsed with saline.

Myocardial tissue preparation

Myocardial tissue near the cardiac apex was harvested and then fixed with 4% paraformaldehyde for 48 h. After fixation, heart tissue was embedded in paraffin and cut into transverse sections (6-μm thickness) for subsequent histological analysis as well as TUNEL and immunohistochemicalstaining.

TUNEL assay

Cardiomyocytes apoptosis in three groups was measured using the TUNEL assay (Roche, Basel, Switzerland, Ca#TUN11684817) according to manufacturer's protocols. The cells with TUNEL-labelled nuclei were regarded as TUNEL-positive cells, and DAPI labelled all cell nuclei. For each slide, 5 microscopic fields (200×) were randomly selected to count TUNEL-positive cells and the total number of cells; the TUNEL staining ratio was calculated as the number of apoptotic cardiomyocytes vs. total myocytes.

Immunohistochemicalstaining

The paraffin slides were dewaxed, and endogenous peroxidase activity was blocked by incubation with methanol containing 1.5% H_2O_2 for 15 min. Then, the slides were washed three times with PBS. Antigen retrieval was achieved by boiling the tissues in citrate saline (pH 6.0) solution for 20 min. These slides were washed with PBS again. Next, 5% goat serum was used to blot the tissues for 30 min at 37°C, and the slides were incubated with primary antibodies, such as rabbit LC3B (1:150), at 4°C overnight. On the next day, the slides were treated with goat anti-rabbit IgG secondary antibody for 30 min at 37°C.Then, the

slides were washed with PBS and incubated with horseradish enzyme tag chain enzyme avidin working solution for 30 min at 37°C. After washing, the slides were dipped into 3-3'diaminobenzidine, at which time the target protein LC3B could be visualized by fluorescence microscopy. Haematoxylin was used as the counterstaining reagent. These slides were then dried, cover slipped and examined under a microscope. The relative Optical Density (ROD) was calculated by image pro plus software as the ratio of the Integral Optical Density (IOD) vs.the measured area.

Myocardial infarct size measurements

Another three groups of rats were established as described above (n=4 per group). Myocardial infarct size was detected by TTC and Evans blue dye staining. After 24 h of reperfusion, 2% Evans Blue dye was injected into the aorta. Then, the hearts were quickly frozen at -70°C and cut into 2-mm thick slices. The slices were stained with 1%TTC at room temperature for 30 min. The area stained blue by Evans blue indicated the area not at risk, whereas the unstained tissues represented AAR. AAR but viable tissue was stained red by TTC, while the infracted myocardium was not stained by any dye and appeared more white than other areas. IS was calculated by image pro plus software as the ratio of IS vs. AAR.

Echocardiography

After 7 days of reperfusion, cardiac function was detected in rats assigned to the three groups by transthoracic echocardiography using a Visual Sonics Vevo 2100 system with a Ms-400 linear transducer (Visual Sonics Vevo 2100, Toronto, CA)(n=4pergroup). EF and LVFS were measured. All results were obtained from five consecutive cardiac cycles.

Statistical analysis

All results are presented as the mean±SD. Statistical analysis was performed using SPSS software 19.0 (SPSS Inc., Chicago, IL, USA). Statistical significance was determined by one-way ANOVA followed by a post hoc Tukey's test or two-way ANOVA followed by a post hoc Bonferroni test. $P < 0.05$ was considered statistically significant.

Results

H_2O_2 induced ROS generation and reduced cell viability in H9C2s

Several mechanisms are involved in MIRI, including energy metabolism disorders, neutrophil infiltration, calcium overload, vascular endothelial dysfunction [18] and ROS overproduction [19]. Therefore, H_2O_2-stimulated H9C2s were used as a model for ROS overproduction, thus mimicking MIRI. Compared with cells in the control group, H_2O_2 induced a dose-dependent decrease in cell viability, as measured by CCK-8 in H9C2s at 3 h, 6 h and 12 h; the effect peaked at 12 h for all concentrations tested (Fig. 1A). H9C2 cell viability was reduced to 50% at 12 h by 500μM H_2O_2 (Fig. 1A), and this concentration was therefore chosen for subsequent experiments. After exposure to H_2O_2, ROS production in H9C2s increased in a dose-dependent manner at 3 h, 6 h and 12 h (Fig. 1B). Additionally, mean fluorescence intensities of di-chlorodihydrofluorescein diacetate (DCFA) significantly increased at 6 h and 12 h in H9C2s post H_2O_2 (Fig. 1C).To verify if the effects on H9C2 cell survival were caused by ROS, the abovementioned experiments were performed in the presence of an antioxidant, N-acetyl cysteine (NAC). Compared with the H_2O_2 group (12 h, 500 μM), ROS production, mean fluorescence intensities of DCFA (Fig. 1D, E), and cell apoptosis (Fig. 1F) were significantly reduced in the H_2O_2+NAC group. The results therefore suggested that H_2O_2-induced ROS generation in H9C2s was responsible for the reduced cell viability.

Changes in autophagy and apoptosis in H9C2s post H_2O_2 stimulation at different time points

To gain insight into mechanisms underlying changes in autophagy in H9C2s after exposure to H_2O_2, autophagy proteins, LC3B and Beclin-1 were detected at 3 h, 6 h and 12

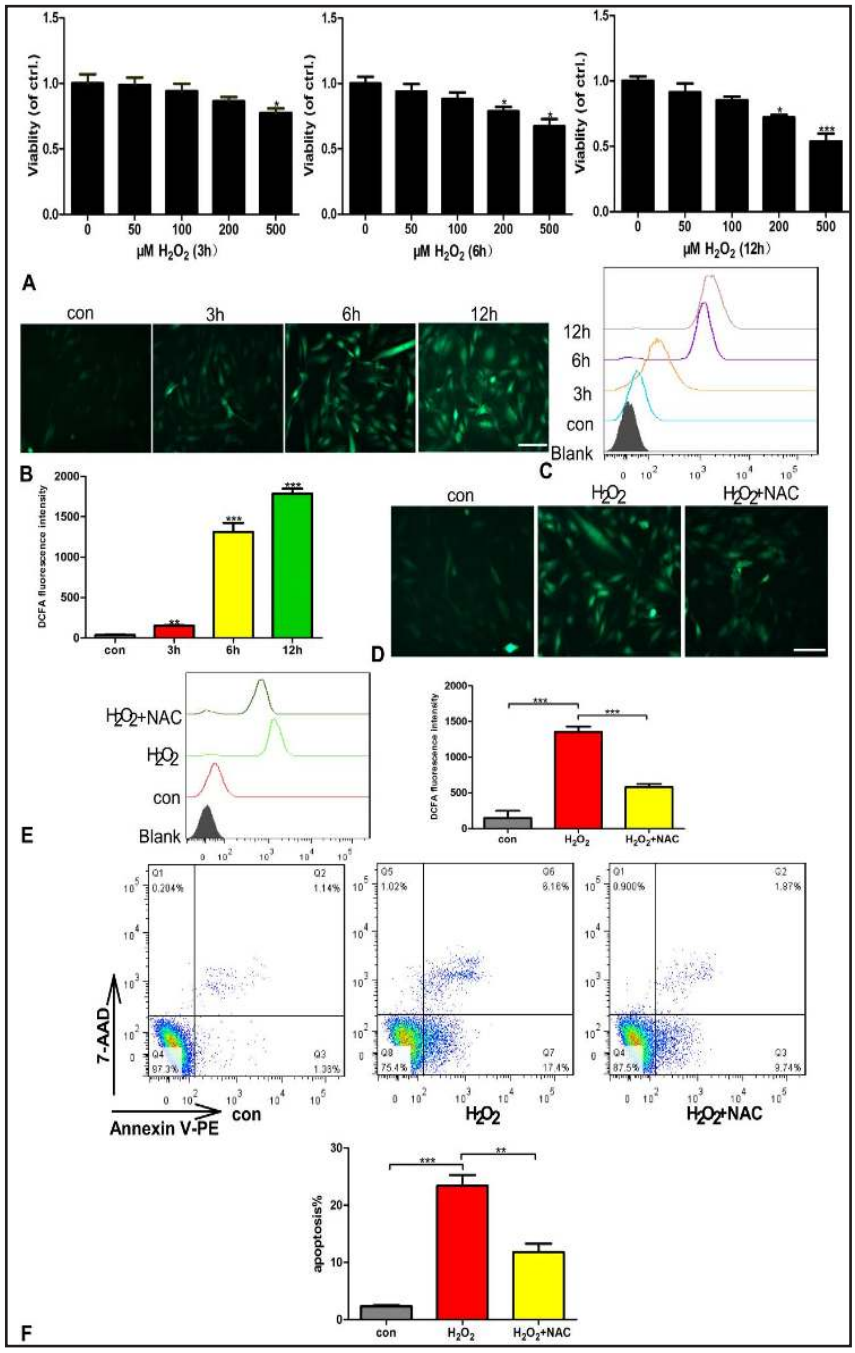

Fig. 1. H_2O_2 induced ROS generation and inhibited cell viability in H9C2s. (A). CCK-8 was used to measure H9C2 cell viability after exposure to 50,100,200 and 500 μM H_2O_2 for 3 h, 6 h and 12 h. (B-C). ROS generation induced by H_2O_2 (500 μM) at 3 h, 6 h and 12 h was detected by fluorescence microscopy and FCM. (D-E). NAC, an antioxidant, reduced the ROS generation induced by H_2O_2 (500 μM) exposure for 12 h, as detected by fluorescence microscopy and FCM. (F). H9C2 cell apoptosis increased after exposure to H_2O_2 (500 μM) for 12 h, and the apoptotic effect was ameliorated by NAC, as detected by FCM. Each bar represents the mean±SD of three independent experiments. Transverse line=100μm. *P<0.05; **P<0.01; and ***P<0.001 compared with the control group.

h after H_2O_2 (500 μM) stimulation. LC3B-II protein levels were significantly increased at 3 h and then decreased at 6 h and 12 h (Fig. 2A). Similar results were obtained for Beclin-1 (Fig. 2A). p62, a marker of degeneration of autophagy, was also detected. P62 protein levels significantly increased at 3 h, reduced at 6 h and then increased at 12 h post H_2O_2 exposure, but its level remained lower than that in the control condition (Fig. 2A). Levels of the apoptosis-related proteins Bcl-2 and Bax [20] were analysed; the former declined and the latter increased after H_2O_2 exposure in a time-dependent manner (Fig. 2B). Moreover, levels of LC3B-II and Beclin-1 as well as the Bcl-2/Bax ratio were significantly higher and levels of p62 were significantly lower in the H_2O_2+NAC group compared with the H_20_2-only group at 12 h after their respective treatments (Fig. 2C, D). The aforementioned results suggested

that H_2O_2-induced cell autophagic flux appeared to be harmful at the early phase but may be beneficial at a later phase.

MSC-derived exosomes: Characterization and internalization into H9C2s

The exosomes were present in larger quantities in the supernatant fluids of MSCs after 24 h of H_2O_2 exposure (Fig. 3A). qNano analysis showed that most MSC-derived exosomes were50-150 nm in diameter (Fig. 3B). The concentration of exosome particles from supernatant fluids of MSCs after 24 h of H_2O_2 stimulation tended to be higher compared that after12 h of H_2O_2 stimulation (Fig. 3B). Most PKH26-labeled exosomes were localized in the cytoplasm of H9C2s at 12 h post H_2O_2 stimulation (Fig. 3C). These data suggested that MSC-derived exosomes could be internalized into H9C2s post H_2O_2 stimulation.

MSC-derived exosomes enhanced H9C2 cell viability and reduced cell apoptosis and ROS production after H_2O_2 stimulation

Compared to the H_2O_2-only group, cell viability was significantly increased (Fig. 4A), ROS production was dramatically decreased (Fig. 4B, C) and the cell apoptosis ratio was significantly reduced (Fig. 4D) in the H_2O_2+exosomes group.

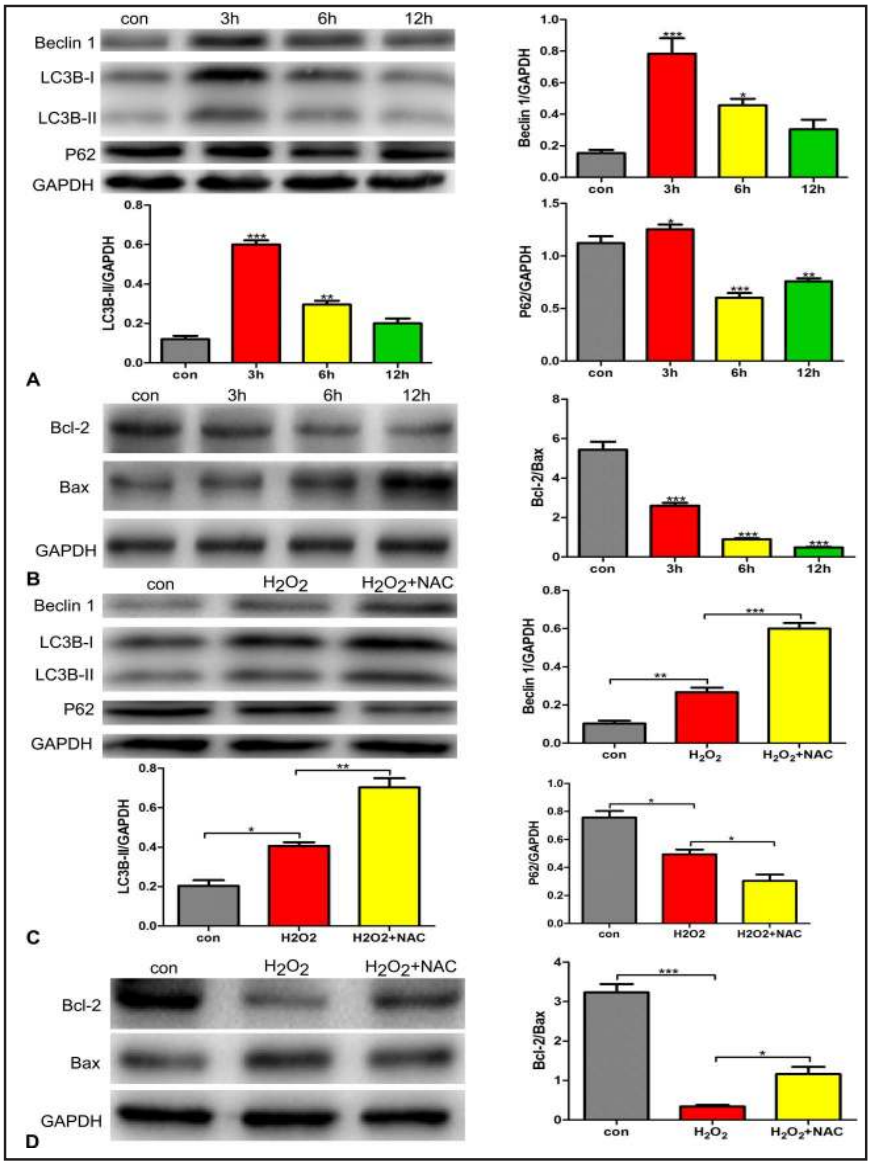

Fig. 2. Changes in H_2O_2-induced autophagy and apoptosis in H9C2s at different time points. (A). WB was used to detect H_2O_2 (500 μM)-induced changes in autophagy proteins, LC3B, Beclin-1 and p62, at3 h, 6 h and 12 h. (B). WB was used to detect H_2O_2 (500 μM)-induced changes in apoptosis-related proteins, Bcl-2 and Bax, at 3 h, 6 h and 12 h. (C). NAC counteracted the H_2O_2 (500 μM)-induced reduction in cell autophagy proteins at 12 h. (D). NAC restored the H_2O_2 (500 μM) induced change in the Bcl-2/Bax ratio at 12 h. Each bar represents the mean±SD of three independent experiments. *P<0.05; **P<0.01; and ***P<0.001 compared to the control group.

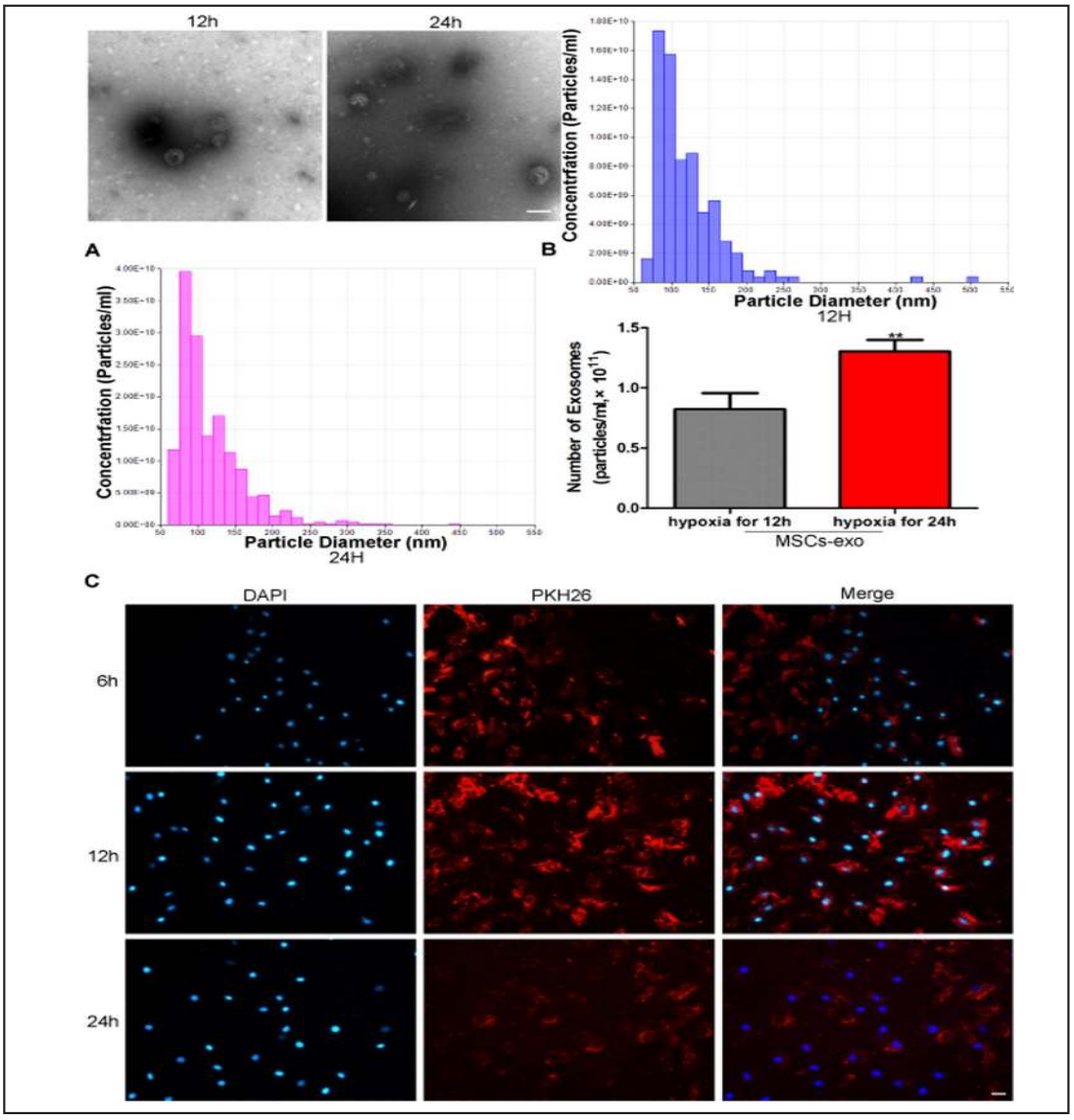

Fig. 3. Characterization of MSC-derived exosomes, and their internalization into H9C2s. (A). Exosomes extracted using the ExoQuick method from the supernatant fluids after incubating MSCs in hypoxic conditions for 12 h or 24 h were examined using TEM. (B). qNano was used to measure the size distribution and concentration of MSC-derived exosomes. (C). The internalization of exosomes into H9C2s was detected by fluorescence microscopy after H9C2s were co-cultured with PKH26-labeled exosomes for 6 h, 12 h and 24 h. Transverse line=100μm. Each bar represents the mean±SD of three independent experiments. *P<0.05 as compared to the control group, and three independent experiments were performed in A and B.

MSC-derived exosomes increased the level of H9C2 cell autophagy

To observe the effects of exosomes on cell autophagy, Bafilomycin A1 (Baf-A1) was used to inhibit autophagy. Compared with the H_2O_2-only group, the expression of Beclin-1 and LC3B-II was significantly enhanced (both $p<0.01$) and the expression of p62 was significantly decreased in the H_2O_2+exosomes group ($p<0.001$) (Fig. 5A), whereas the levels of LC3B-II, Beclin-1 and p62 were higher in the H_2O_2+exosomes+Baf-A1 group compared with the H_2O_2+exosomes group (Fig. 5A). Compared with the H_2O_2 exposure group, both autophagosomes and autolysosomes were significantly increased in the exosome-treated

group (Fig. 5B).Although the levels of autophagosomes were significantly enhanced in the H_2O_2+exosomes+Baf-A1 group, they were not increased compared with the H_2O_2+exosomes group (Fig. 5B). Autophagosomes detected by TEM were similar as that detected by double fluorescent mRFP-GFP-LC3 (Fig. 5C). As described above, enhancement of autophagy in H9C2s at 12 h after H_2O_2 exposure could reduce apoptosis. Therefore, increased cell autophagy induced by MSC-derived exosomes might serve as an important mechanism responsible for their cytoprotective effects after H_2O_2 stimulation.

MSC-derived exosomes regulate cell autophagy via AMPK/mTOR and Akt/mTOR signalling

Cell autophagy is known to be associated with many signalling pathways, and the involvement of AMPK/mTOR and Akt/mTOR signalling has been documented in MIRI [21-23]. We assessed whether MSC-derived exosome-regulated autophagy was partly mediated through the latter two pathways. Our results showed that p-mTOR/mTOR and p-Akt/Akt

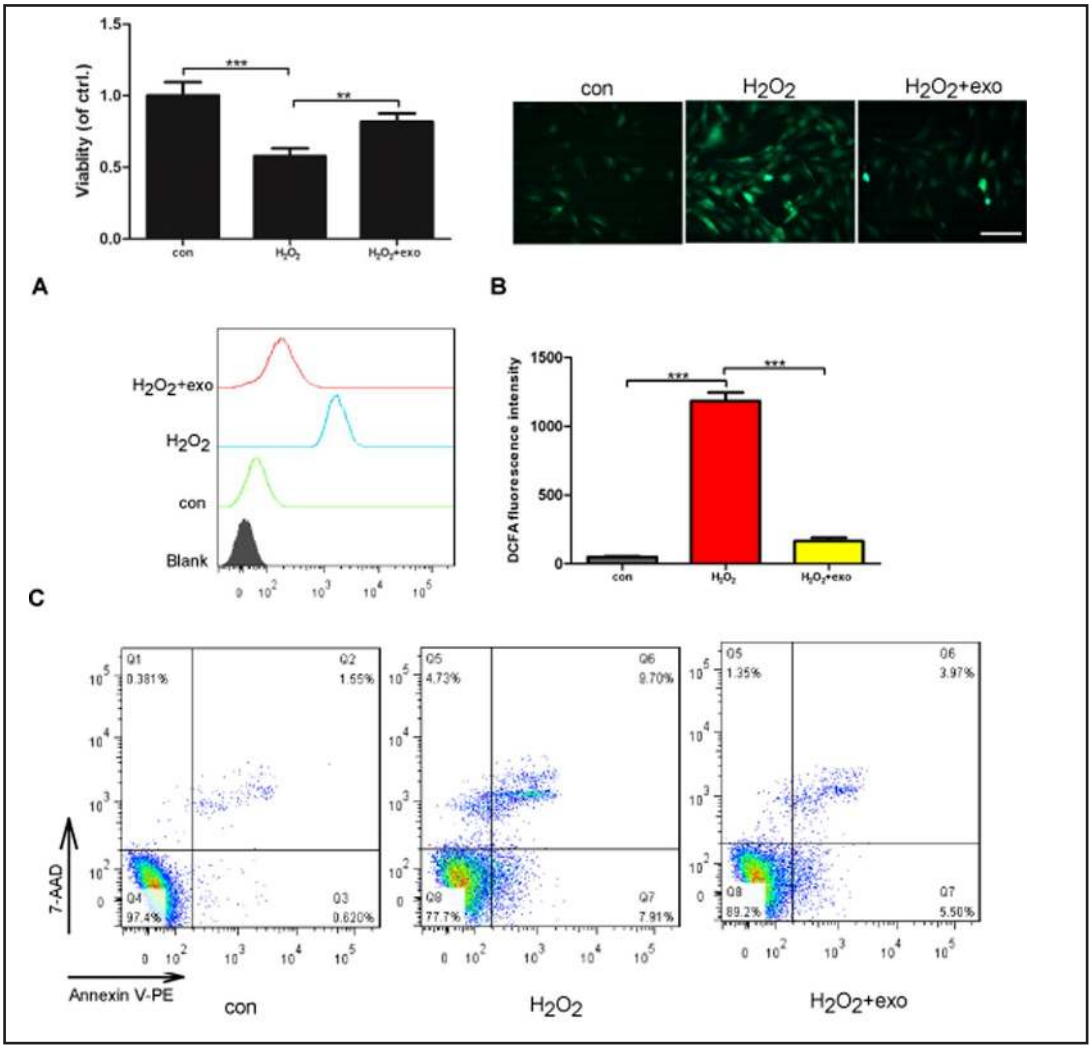

Fig. 4. MSC-derived exosomes enhanced H9C2 cell viability and reduced the cell apoptosis and ROS production induced by H_2O_2. Three groups were studied: control cells; cells exposed to H_2O_2 (500 μM) for 12 h; and cells co-cultured with exosomes (10 μg/ml) for 12 h prior to exposure to H_2O_2 (500 μM) for 12 h. (A). Cell viability was assessed by CCK-8. (B-C). ROS production was measured by fluorescence microscopy and FCM. (D). H9C2 cell apoptosis was tested by FCM. Each bar represents the mean±SD of three independent experiments. Transverse line=100μm. exo=exosomes. *P<0.05; and ***P<0.001 compared to the control group.

expression levels were significantly lower in the H_2O_2+exosomes group than in the H_2O_2-only group and that this effect could be reversed by co-treatment with 3-methyladenine(3-MA), an autophagy inhibitor (Fig. 6A). p-AMPK/AMPK expression was significantly higher in the H_2O_2+exosomes group than in the H_2O_2-only group. Compound C (CC), an AMPK inhibitor, was used to assess the role of AMPK signalling in exosome-regulated cell autophagy. Cells were divided into four groups (control, H_2O_2, H_2O_2+exosomes and H_2O_2+exosomes+CC). p-mTOR/mTOR was dramatically enhanced, whereas p-AMPK/AMPK,LC3B-II and Beclin-1

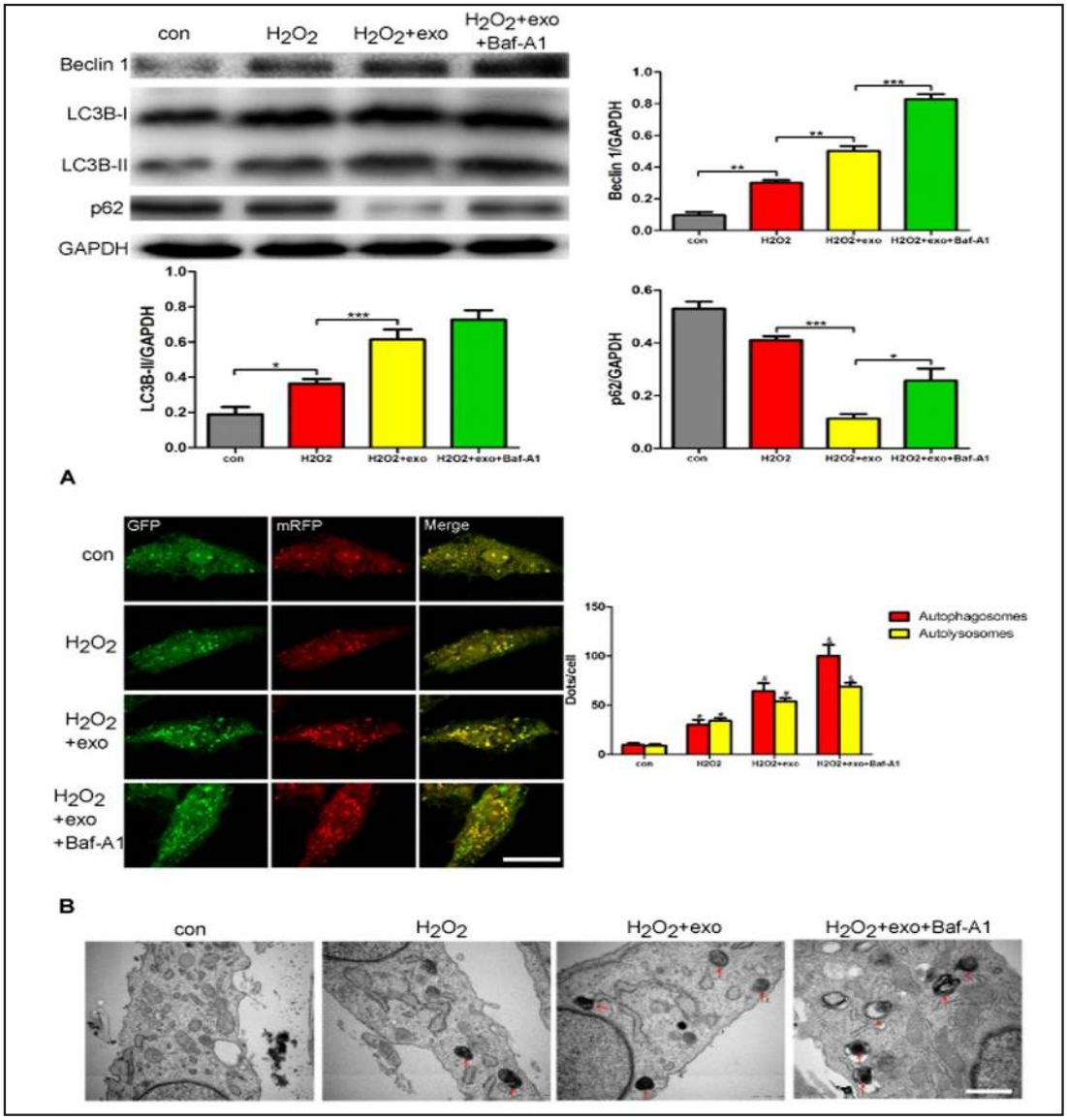

Fig. 5. MSC-derived exosomes increased the level of H9C2 cell autophagy. The four groups studied were as follows: control cells; cells exposed to H_2O_2 (500 μM) for 12 h; cells co-cultured with exosomes (10 μg/ml) for 12 h prior to exposure to H_2O_2 (500 μM) for 12 h; and cells co-cultured with exosomes (10 μg/ml) for 12 h prior to exposure to Baf-A1 for 1 h and then H_2O_2 (500 μM) exposure for 12 h. (A). LC3B, Beclin-1 and p62, were detected by WB. (B). Autophagosomes and autolysosomes were detected by tandem fluorescent mRFG-GFP-LC3 assay. *p<0.05 vs. the control group; #p<0.05 vs. the H_2O_2 group; and $p<0.05 vs. the H_2O_2 +exo group. C. Autophagosomes were measured by TEM in four groups. Each bar represents the mean±SD of three independent experiments. Transverse line=100μm. exo=exosomes.*P<0.05; and ***P<0.001 compared to the control group.

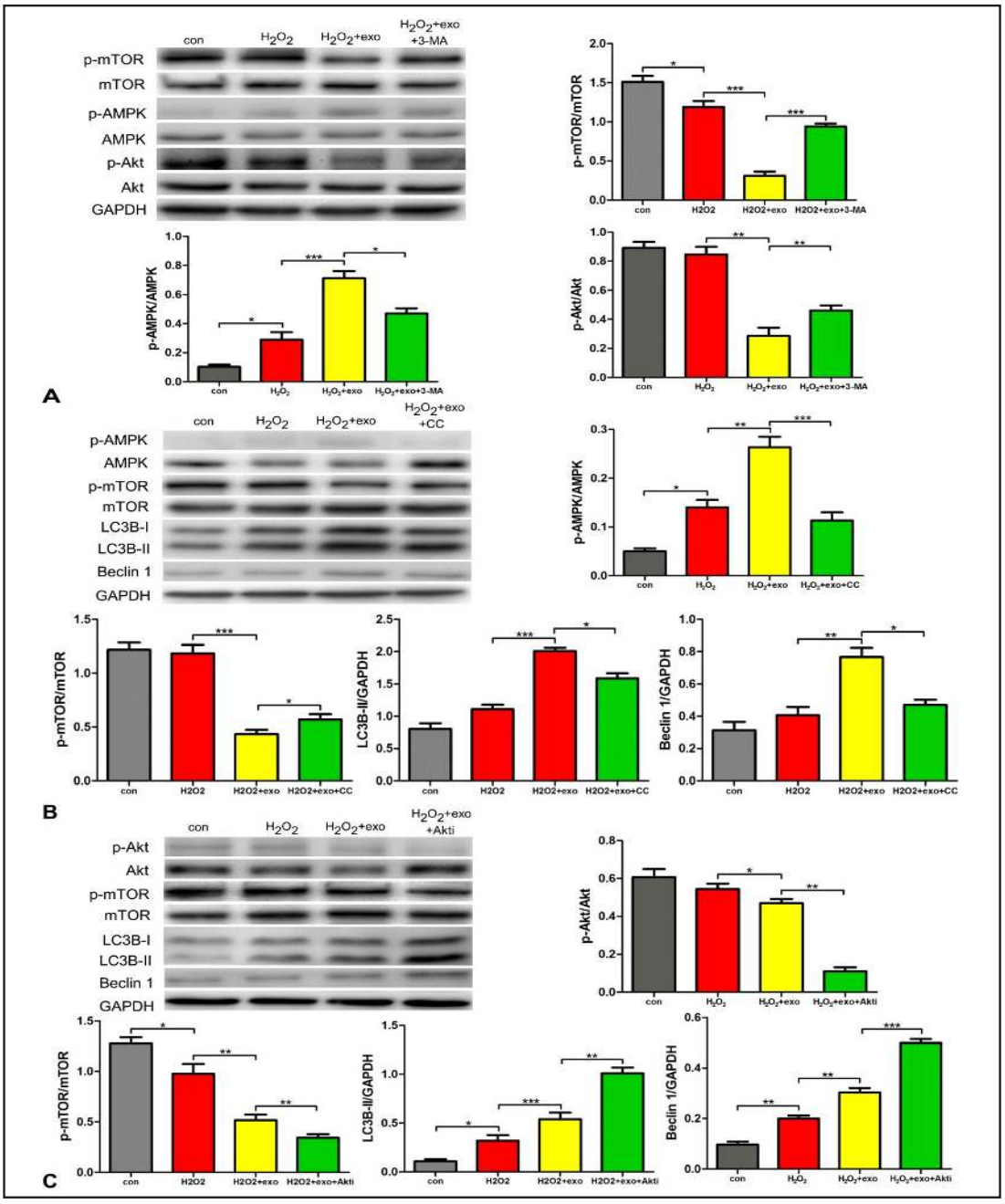

Fig. 6. MSC-derived exosomes regulate cell autophagy via AMPK/mTOR and Akt/mTOR signalling. (A).p-mTOR/mTOR, p-AMPK/AMPK and p-Akt/Akt were detected by WB in four groups: the control group, the H_2O_2-only group, the H_2O_2+exosomes group, and the H_2O_2+exosomes+3-MA group. (B). p-AMPK/AMPK, p-mTOR/mTOR,LC3B and Beclin 1 were detected by WB in four groups: the control group, the H_2O_2-only group, the H_2O_2+exosomes group, and the H_2O_2+exosomes+CC group.(C). p-Akt/Akt, p-mTOR/mTOR,LC3B and Beclin 1 were detected by WB in four groups: the control group, the H_2O_2-only group, the H_2O_2+exosomes group, and the H_2O_2+exosomes+Akti group. Each bar represents the mean±SD of three independent experiments. exo=exosomes. *P<0.05; and ***P<0.001 compared to the control group.

expression tended to be lower in the CC group compared to that in the exosome-treated group after cells in both groups were exposed to H_2O_2 (500 μM) for 12 h (Fig. 6B). Akti,

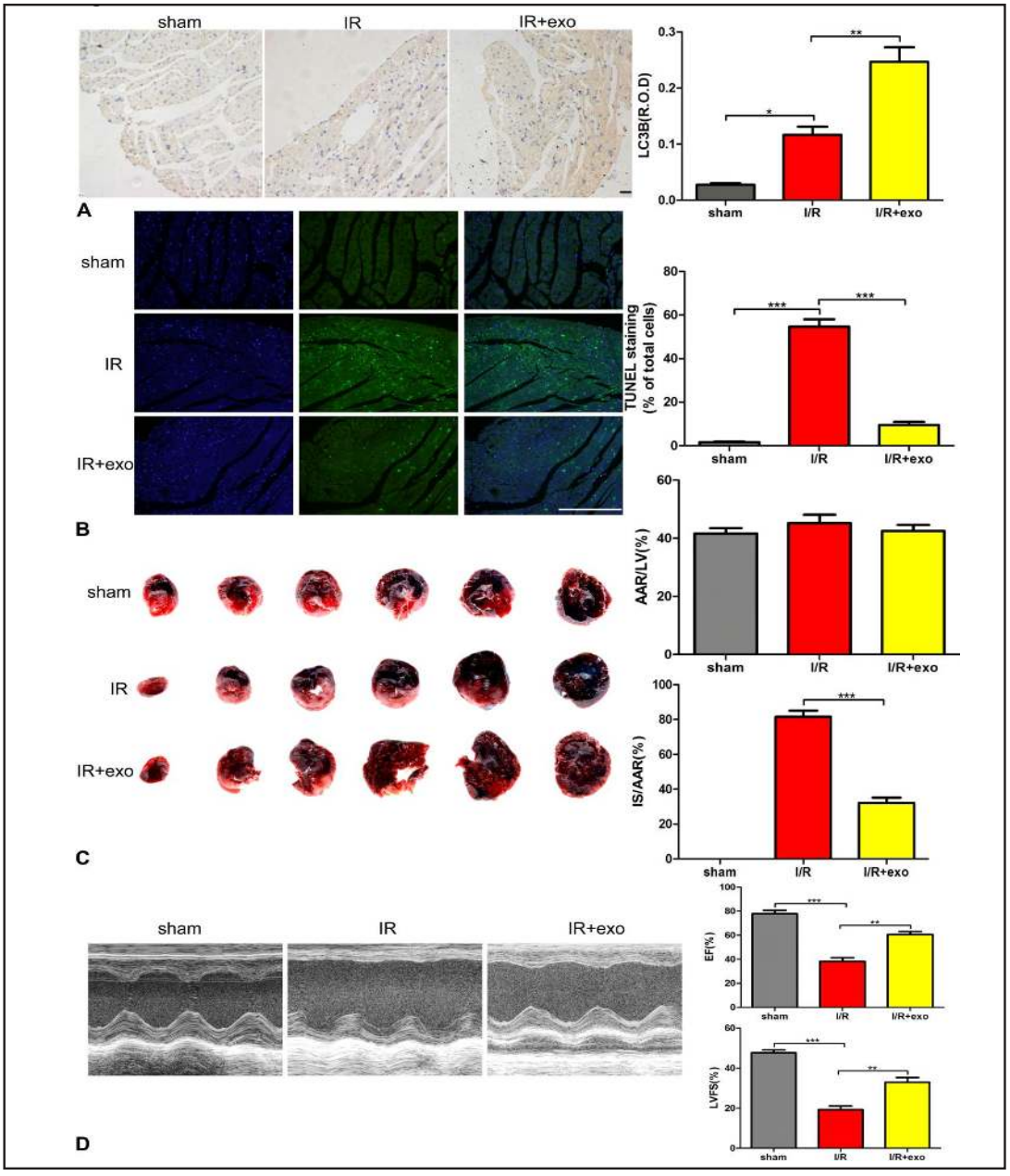

Fig. 7. Autophagy induced by MSC-derived exosomes decreased rat cardiomyocyte apoptosis and the myocardial infarction size as well as improved heart function *in vivo*. (A). LC3B was detected in myocardial tissue by fluorescence microscopy. ROD was calculated by image pro plus software as the ratio of IOD vs.the measured area. (B). Cardiomyocyte apoptosis in myocardial tissue was measured using the TUNEL assay. The TUNEL staining ratio was calculated as the ratio of apoptotic cardiomyocytes vs. total myocytes. (C). Myocardial infarction size was detected by TTC/Evan blue staining. Blue, red and white stained areas represent viable myocardium, AAR and IS, respectively. AAR/LV and IS/AAR were calculated by image pro plus software. (D). The heart function of rats in the four groups was measured by echocardiography. Each bar represents the mean±SD of four or six independent experiments. Transverse line=100μm. exo=exosomes.*P<0.05; and ***P<0.001 compared to the control group.

an Akt inhibitor, was also used to assess if exosomes affected autophagy via the Akt/mTOR pathway. Cells were divided into four groups (control, H_2O_2, H_2O_2+exosomes and

H_2O_2+exosomes+Akti). Compared to the H_2O_2-only group and the H_2O_2+exosomes group, a significantly reduced p-mTOR/mTOR ratio and enhanced cell autophagy were evidenced in the H_2O_2+exosomes+Akti group (Fig. 6C). Therefore, the above results indicated that the enhanced MSC-derived exosome-induced H9C2 cell autophagy after exposure to H_2O_2 was at least partly mediated by the AMPK/mTOR and Akt/mTOR signalling pathways.

Autophagy induced by MSC-derived exosomes decreased rat cardiomyocyte apoptosis and the myocardial infarction size and improved heart function in vivo

Compared with the control group, LC3B expression was significantly enhanced (Fig. 7A) and cardiomyocyte apoptosis, as detected by the TUNEL assay (Fig. 7B), was significantly reduced in the infarct area of I/R rats treated with myocardial exosomes. The infarction size (IS) in the exosome-treated group was also significantly reduced compared with that in untreated I/R rats (Fig. 7C). The ejection fraction (EF) and left ventricular fractional shortening (LVFS) in I/R rats treated with exosomes were significantly higher than that in untreated I/R rats after 7 days of reperfusion (Fig. 7D).

Discussion

The present study documented that MSC-derived exosomes enhanced autophagy and reduced cell apoptosis and ROS production in H9C2s stimulated by H_2O_2. Likewise, when MSC-derived exosomes were injected into the *in vivo* MIRI rat model, autophagy was increased, apoptosis and the myocardial infarction size were reduced, and cardiac function was improved. Our experiments also demonstrated that the above effects were partly mediated through AMPK/mTOR and Akt/mTOR signalling. To our knowledge, the present study was the first to document that MSC-derived exosomes could protect against H_2O_2-induced injury in H9C2 cells by enhancing autophagy.

Many studies have demonstrated excess ROS production during MIRI, mainly from the mitochondrial transport chain [24, 25]. Excessive ROS leads to cell death by various mechanisms, including direct injury to biomolecules (lipids, proteins and DNA) or indirect injury by the activation of pro-apoptotic pathways [26]. In line with previous studies, we showed that H_2O_2-induced ROS reduced H9C2 cell viability and increased H9C2 cell apoptosis. The latter effects of ROS were reversed by the antioxidant NAC.

Several studies have demonstrated that enhanced autophagy post-hypoxia or ischaemic injury has a myocardial protective effect [27, 28]. Excessive ROS production during the reperfusion stage post-ischaemia can lead to cell autophagy dysfunction. A previous study showed that moderate myocardial autophagy reduced myocardial apoptosis and improved myocardial cell survival, whereas excessive autophagy may aggravate myocardial damage [29]; many other studies have demonstrated that upregulation of autophagy in cardiomyocytes attenuated MIRI [22, 30, 31]. Matsui et al. reported a beneficial effect from myocardial autophagy induced by AMPK pathway activation; however, during the reperfusion stage, excessive autophagy induced by Beclin-1 pathway activation could lead to cell death [32]. It was also shown that during the reperfusion stage, partial Beclin-1 knockdown could reduce reoxygenation-induced cardiomyocyte cell death, whereas full Beclin-1 knockdown reduced autophagosome formation and increased cell death [33]. Therefore, the effects of ROS-induced autophagy are multi-faceted. In the present study, autophagic flux was blocked in H9C2s after exposure to H_2O_2 for 3 h; additionally, autophagy was decreased at 6 h and 12 h, which is consistent with a time-dependent decrease in the proliferation-related Bcl-2 and apoptosis-related Bax ratio. The antioxidant NAC enhanced H_2O_2-induced autophagy in H9C2s at 12 h and reversed the Bcl-2/Bax ratio at 12 h. The latter results may provide new insight into the various effects caused by ROS on autophagy, namely, that autophagy dysfunction at an early stage appears to be harmful, whereas enhanced moderate autophagy at a later stage appears to be beneficial.

Several studies have documented that exosomes derived from MSCs have therapeutic potential by improving cardiacfunction after hypoxia *in vitro* or myocardial infarction *in*

vivo [34-36]; treatment with exosomes reduce the myocardial infarction area and improve cardiac function in I/R animal models [10, 11]. However, the underlying mechanisms remain elusive. The present study documented that MSC-derived exosomes not only reduced H_2O_2-induced ROS production and apoptosis *in vitro* but also reduced myocardial cell apoptosis and myocardial infarction size and improved heart function following MIRI *in vivo*. To the best of our knowledge, this is the first report of the beneficial effects of MSC-derived exosomes *in vitro*. One study showed that MSC-derived exosomes activated the PI3K/Akt pathway to prevent myocardial remodelling post-MIRI *in vivo* [11]. The PI3K/Akt pathway is a common autophagy signalling pathway [37]. Another report showed that a reduction of cardiomyocyte-derived exosome release during hypoxia enhanced autophagy in cardiomyocytes and reduced cardiomyocyte apoptosis caused by hypoxia *in vitro* [38]. The latter *in vivo* and *in vitro* studies hinted that autophagy in H9C2s may be linked to an MSC-derived exosome-mediated protective mechanism. In fact, we showed, in the present study that compared with exposure to H_2O_2 alone, treatment with MSC-derived exosomes significantly enhanced H9C2 cell autophagy and reduced the Bcl-2/Bax ratio. Moreover, autophagy in rat myocardial cells was enhanced after an *in vivo* rat I/R model was injected with exosomes. The aforementioned findings thus provide novel insight into the treatment mechanism of exosomes in MIRI.

In the present study, we demonstrated that exosomes enhanced the p-AMPK/AMPK ratio and reduced the p-Akt/Akt and p-mTOR/mTOR ratios in H9C2s after exposure to H_2O_2 for 12 h, suggesting that the AMPK/mTOR and Akt/mTOR pathways may actively participate in these processes. Accordingly, previous research has shown that restoration of autophagic flux in cardiomyocytes by activating the AMPK pathway reduced MIRI [39]. Another study also demonstrated that autophagy was enhanced in H9C2s following AMPK/mTOR activation and had protective effects on cells during hypoxia/reoxygenation injury [40]. In the present study, AMPK inhibition by CC also reversed the exosome-mediated increase in the expression of LC3B-II and Beclin-1 and decreased the expression of p-mTOR /mTOR, suggesting that autophagy enhancement in H9C2s by MSC-derived exosomes after exposure to H_2O_2 was at least partly mediated by modulating the AMPK/mTOR pathway. Our finding is in line with that of previous *in vivo* and *vitro* studies, showing that Akt/mTOR-regulated autophagy in cardiomyocytes actively participates in hypoxia/reoxygenation injury or MIRI in animal models [11, 41]. In the present study, Akt inhibition significantly reduced the p-mTOR/mTOR ratio and enhanced cell autophagy, suggesting that MSC-derived exosome-enhanced autophagy in H9C2s after exposure to H_2O_2 is at least partly mediated by modulating the Akt/mTOR pathway.

Conclusion

The findings of the present study provide new insight into the therapeutic effect of MSC-derived exosomes after H_2O_2exposure in H9C2 cells and indicate the important role of autophagy in mediating the beneficial effects of exosomes on MIRI. Many studies have found that miRNAs or proteins in the exosomes play a major role in many disease models [42, 43]. Therefore, additional experiments are warranted to determine the role of individual RNA, miRNA and related protein elements of exosomes and to validate their individual roles in the effects described above.

Acknowledgements

This work was supported by the Nature Science Foundation of China Grant 81470470 and the Shanghai Medical Key Specialty Construction Projects (Class A, series number: ZK2012A24). We thank Dr. Kai Hu from the Würzburg University in Germany for his help with the preparation of this manuscript.

Disclosure Statement

None.

References

1 Murray CJ, Lopez AD: Alternative projections of mortality and disability by cause 1990-2020: Global Burden of Disease Study. Lancet 1997;349:1498-1504.
2 Binder A, Ali A, Chawla R, Aziz HA, Abbate A, Jovin IS: Myocardial protection from ischemia-reperfusion injury post coronary revascularization. Expert Rev Cardiovasc Ther 2015;13:1045-1057.
3 Bresnahan GF, Roberts R, Shell WE, Ross J, Jr., Sobel BE: Deleterious effects due to hemorrhage after myocardial reperfusion. Am J Cardiol 1974;33:82-86.
4 Xu Y, Huo Y, Toufektsian MC, Ramos SI, Ma Y, Tejani AD, French BA, Yang Z: Activated platelets contribute importantly to myocardial reperfusion injury. Am J Physiol Heart Circ Physiol 2006;290:H692-699.
5 Pfister O, Della Verde G, Liao R, Kuster GM: Regenerative therapy for cardiovascular disease. Transl Res 2014;163:307-320.
6 Li Q, Wang Y, Deng Z: Pre-conditioned mesenchymal stem cells: a better way for cell-based therapy. Stem Cell Res Ther 2013;4:63.
7 Phinney DG, Prockop DJ: Concise review: mesenchymal stem/multipotent stromal cells: the state of transdifferentiation and modes of tissue repair--current views. Stem Cells 2007;25:2896-2902.
8 Caplan AI, Dennis JE: Mesenchymal stem cells as trophic mediators. J Cell Biochem 2006;98:1076-1084.
9 Thery C, Ostrowski M, Segura E: Membrane vesicles as conveyors of immune responses. Nat Rev Immunol 2009;9:581-593.
10 Lai RC, Arslan F, Lee MM, Sze NS, Choo A, Chen TS, Salto-Tellez M, Timmers L, Lee CN, El Oakley RM, Pasterkamp G, de Kleijn DP, Lim SK: Exosome secreted by MSC reduces myocardial ischemia/reperfusion injury. Stem Cell Res 2010;4:214-222.
11 Arslan F, Lai RC, Smeets MB, Akeroyd L, Choo A, Aguor EN, Timmers L, van Rijen HV, Doevendans PA, Pasterkamp G, Lim SK, de Kleijn DP: Mesenchymal stem cell-derived exosomes increase ATP levels, decrease oxidative stress and activate PI3K/Akt pathway to enhance myocardial viability and prevent adverse remodeling after myocardial ischemia/reperfusion injury. Stem Cell Res 2013;10:301-312.
12 Akyurekli C, Le Y, Richardson RB, Fergusson D, Tay J, Allan DS: A systematic review of preclinical studies on the therapeutic potential of mesenchymal stromal cell-derived microvesicles. Stem Cell Rev 2015;11:150-160.
13 Yu B, Zhang X, Li X: Exosomes derived from mesenchymal stem cells. Int J Mol Sci 2014;15:4142-4157.
14 Levine B, Klionsky DJ: Development by self-digestion: molecular mechanisms and biological functions of autophagy. Dev Cell 2004;6:463-477.
15 Belanger M, Rodrigues PH, Dunn WA, Jr., Progulske-Fox A: Autophagy: a highway for Porphyromonas gingivalis in endothelial cells. Autophagy 2006;2:165-170.
16 Dosenko VE, Nagibin VS, Tumanovska LV, Moibenko AA: Protective effect of autophagy in anoxia-reoxygenation of isolated cardiomyocyte? Autophagy 2006;2:305-306.
17 Qiao S, Xie H, Wang C, Wu X, Liu H, Liu C: Delayed anesthetic preconditioning protects against myocardial infarction via activation of nuclear factor-kappaB and upregulation of autophagy. J Anesth 2013;27:251-260.
18 Turer AT, Hill JA: Pathogenesis of myocardial ischemia-reperfusion injury and rationale for therapy. Am J Cardiol 2010;106:360-368.
19 Windecker S, Bax JJ, Myat A, Stone GW, Marber MS: Future treatment strategies in ST-segment elevation myocardial infarction. Lancet 2013;382:644-657.
20 Volkmann N, Marassi FM, Newmeyer DD, Hanein D: The rheostat in the membrane: BCL-2 family proteins and apoptosis. Cell Death Differ 2014;21:206-215.
21 Zhang Y, Ren J: Autophagy in ALDH2-elicited cardioprotection against ischemic heart disease: slayer or savior? Autophagy 2010;6:1212-1213.
22 Mo Y, Tang L, Ma Y, Wu S: Pramipexole pretreatment attenuates myocardial ischemia/reperfusion injury through upregulation of autophagy. Biochem Biophys Res Commun 2016;473:1119-1124.
23 Wu X, He L, Cai Y, Zhang G, He Y, Zhang Z, He X, He Y, Zhang G, Luo J: Induction of autophagy contributes to the myocardial protection of valsartan against ischemiareperfusion injury. Mol Med Rep 2013;8:1824-1830.

24 Agarwal A, Banerjee A, Banerjee UC: Xanthine oxidoreductase: a journey from purine metabolism to cardiovascular excitation-contraction coupling. Crit Rev Biotechnol 2011;31:264-280.
25 Youn JY, Zhang J, Zhang Y, Chen H, Liu D, Ping P, Weiss JN, Cai H: Oxidative stress in atrial fibrillation: an emerging role of NADPH oxidase. J Mol Cell Cardiol 2013;62:72-79.
26 Alvarez P, Tapia L, Mardones LA, Pedemonte JC, Farias JG, Castillo RL: Cellular mechanisms against ischemia reperfusion injury induced by the use of anesthetic pharmacological agents. Chem Biol Interact 2014;218:89-98.
27 Ma S, Wang Y, Chen Y, Cao F: The role of the autophagy in myocardial ischemia/reperfusion injury. Biochim Biophys Acta 2015;1852:271-276.
28 Lin C, Liu Z, Lu Y, Yao Y, Zhang Y, Ma Z, Kuai M, Sun X, Sun S, Jing Y, Yu L, Li Y, Zhang Q, Bian H: Cardioprotective effect of Salvianolic acid B on acute myocardial infarction by promoting autophagy and neovascularization and inhibiting apoptosis. J Pharm Pharmacol 2016;68:941-952.
29 Hansford RG, Zorov D: Role of mitochondrial calcium transport in the control of substrate oxidation. Mol Cell Biochem 1998;184:359-369.
30 Ling Y, Chen G, Deng Y, Tang H, Ling L, Zhou X, Song X, Yang P, Liu Y, Li Z, Zhao C, Yang Y, Wang X, Kitakaze M, Liao Y, Chen A: Polydatin post-treatment alleviates myocardial ischemia/reperfusion injury by promoting autophagic flux. Clin Sci (Lond) 2016;10.1042/CS20160082
31 Xie M, Kong Y, Tan W, May H, Battiprolu PK, Pedrozo Z, Wang ZV, Morales C, Luo X, Cho G, Jiang N, Jessen ME, Warner JJ, Lavandero S, Gillette TG, Turer AT, Hill JA: Histone deacetylase inhibition blunts ischemia/reperfusion injury by inducing cardiomyocyte autophagy. Circulation 2014;129:1139-1151.
32 Matsui Y, Takagi H, Qu X, Abdellatif M, Sakoda H, Asano T, Levine B, Sadoshima J: Distinct roles of autophagy in the heart during ischemia and reperfusion: roles of AMP-activated protein kinase and Beclin 1 in mediating autophagy. Circ Res 2007;100:914-922.
33 Ma X, Liu H, Foyil SR, Godar RJ, Weinheimer CJ, Diwan A: Autophagy is impaired in cardiac ischemia-reperfusion injury. Autophagy 2012;8:1394-1396.
34 Teng X, Chen L, Chen W, Yang J, Yang Z, Shen Z: Mesenchymal Stem Cell-Derived Exosomes Improve the Microenvironment of Infarcted Myocardium Contributing to Angiogenesis and Anti-Inflammation. Cell Physiol Biochem 2015;37:2415-2424.
35 Bian S, Zhang L, Duan L, Wang X, Min Y, Yu H: Extracellular vesicles derived from human bone marrow mesenchymal stem cells promote angiogenesis in a rat myocardial infarction model. J Mol Med (Berl) 2014;92:387-397.
36 Yu B, Kim HW, Gong M, Wang J, Millard RW, Wang Y, Ashraf M, Xu M: Exosomes secreted from GATA-4 overexpressing mesenchymal stem cells serve as a reservoir of anti-apoptotic microRNAs for cardioprotection. Int J Cardiol 2015;182:349-360.
37 Heras-Sandoval D, Perez-Rojas JM, Hernandez-Damian J, Pedraza-Chaverri J: The role of PI3K/AKT/mTOR pathway in the modulation of autophagy and the clearance of protein aggregates in neurodegeneration. Cell Signal 2014;26:2694-2701.
38 Yang Y, Li Y, Chen X, Cheng X, Liao Y, Yu X: Exosomal transfer of miR-30a between cardiomyocytes regulates autophagy after hypoxia. J Mol Med (Berl) 2016;94:711-724.
39 Xie H, Xu Q, Jia J, Ao G, Sun Y, Hu L, Alkayed NJ, Wang C, Cheng J: Hydrogen sulfide protects against myocardial ischemia and reperfusion injury by activating AMP-activated protein kinase to restore autophagic flux. Biochem Biophys Res Commun 2015;458:632-638.
40 Zhao M, Sun L, Yu XJ, Miao Y, Liu JJ, Wang H, Ren J, Zang WJ: Acetylcholine mediates AMPK-dependent autophagic cytoprotection in H9c2 cells during hypoxia/reoxygenation injury. Cell Physiol Biochem 2013;32:601-613.
41 Liu L, Wu Y, Huang X: Orientin protects myocardial cells against hypoxia-reoxygenation injury through induction of autophagy. Eur J Pharmacol 2016;776:90-98.
42 Tan M, Yan HB, Li JN, Li WK, Fu YY, Chen W, Zhou Z: Thrombin Stimulated Platelet-Derived Exosomes Inhibit Platelet-Derived Growth Factor Receptor-Beta Expression in Vascular Smooth Muscle Cells. Cell Physiol Biochem 2016;38:2348-2365.
43 Jia R, Li J, Rui C, Ji H, Ding H, Lu Y, De W, Sun L: Comparative Proteomic Profile of the Human Umbilical Cord Blood Exosomes between Normal and Preeclampsia Pregnancies with High-Resolution Mass Spectrometry. Cell Physiol Biochem 2015;36:2299-2306.